Journal of Scientific & Industrial Research
Vol. 81, November 2022, pp. 1204-1216
DOI: 10.56042/jsir.v81i11.46354

An Integrated Approach for Fixture Layout Design and Clamping Force Optimization

Michael Thomas Rex F[1]*, Ravindran D[2], Andrews A[1] & Prince Abraham B[1]

[1]Department of Mechanical Engineering, National Engineering College, Kovilpatti 628 503, Tamil Nadu, India

[2]Department of Mechanical Engineering, Thamirabharani Engineering College, Tirunelveli 627 358, Tamil Nadu, India

Received 13 February 2021; revised 20 October 2022; accepted 20 October 2022

Fixture Layout Design (FLD) determines the specific position of locators and clamps to orient and holds the workpiece with respect to a machine tool. The FLD approaches that use Finite Element Analysis (FEA) have been widely used in previous works and have become computationally expensive and specific to a particular problem. Further, the FLD and clamping force optimization were often performed separately by ignoring their interdependence. In the present work, the locators' contact forces are uniformly distributed by suitably varying the fixture layout and clamping force to maximize the part dimensional and form quality. The parametric rigid body model is used to depict the behaviour of the workpiece-fixture system, and it is incorporated with the genetic algorithm to optimize the design variables. A prismatic workpiece with pocket milling operation is considered to validate the proposed methodology. Stability criterion and tool-fixture interference are considered constraints. Subsequently, FEA is used to verify the integrity of the proposed approach. The results infer that the uniform distribution of maximum elastic deformation is achieved due to the uniform distribution of contact forces. The suggested approach is proven effective for designing a milling fixture to manufacture components with high dimensional and form precision.

Keywords: Contact forces, Finite element analysis, Fixture design, Genetic algorithm

Introduction

Optimum Fixture Layout Design (FLD) is essential to ensure the quality of the components produced by the milling process. The selection of the optimum position of locators and clamps are critical factors in FLD. Optimum FLD is expected to cause a uniform distribution of contact forces at locators; thereby, the dimensional and form accuracies of the components are ensured. Also, the clamping force significantly influences the quality of the components, and it has to be optimum and adequate to constrain the movement of the workpiece during machining. The selection of fixture layout and clamping forces are purely based on the skill of the tool designer and are presently being decided on a trial and error basis. Consequently, the dimensional and form qualities of the components are not ensured. Hence, a systematic procedure to determine the optimum fixture layout and the clamping force is essential to obtain the desired quality.

FLD has been explored by many researchers and suggested various methods for the optimization of fixture layout and clamping force. Wan *et al*. presented a fixture design of a weakly-rigid workpiece to reduce the chatter.[1] The Finite Element Analysis (FEA) was used to analyze the dynamic behaviour of the system under machining conditions. Kaya implemented an integrated approach using a Genetic Algorithm (GA) and FEA to determine the optimum fixture layout.[2] Workpiece was modelled as a two-dimensional element in the optimization process. Vishnupriyan *et al*. developed an ANN model to predict the dynamic motion of a prismatic workpiece during the milling process simulation.[3] Rex and Ravindran developed an experiment-based approach for fixture layout design by limiting the workpiece deformation during the milling operation.[4] The ANN model was developed to predict elastic deformation of the workpiece and validated with FEA. The ANN is trained using the deformation data from fixture configurations derived from FEM, and then an empirical model is created. The evolutionary optimization approaches are integrated with a model that can predict deformation. Ramachandran *et al*. developed a fixture layout design approach for minimizing the deformation of the workpiece to perform drilling operations on an engine bracket.[5]

*Author for Correspondence
E-mail: michealrex@hotmail.com

FEA is used to determine the elastic deformation of the workpiece. An empirical model is created using an artificial neural network (ANN). By integrating the cuckoo search algorithm, Yang *et al*. adopted the FEA-ANN approach for optimum fixture locating layout for sheet metal parts.[6] Lu and Zhao developed ANN-based predictive models to predict the elastic deformation of the workpiece using FEA results.[7] Wu *et al*. developed FEA-based machining fixture-evaluation criteria for a CNC machining process to predict overall deformation, maximum deformation, and system stiffness.[8] Arunraja *et al*. implemented an FEA-based approach to minimize the maximum elastic deformation of the sheet metal workpiece due to the clamping and welding forces.[9] Li *et al*. modelled the workpiece-fixture system as a variable stiffness structure in FEA.[10] To minimize the maximum deformation of the surface to be machined. A face milling experiment on a four-cylinder engine block is used to demonstrate the efficacy and efficiency of the suggested approach.

Chen *et al*. developed a reconfigurable fixture with the aid of the N-M approach to hold the vehicle dashboard.[11] FEA is used to analyze the component for predicting maximum deformation. Rex *et al*. implemented an FEA-based method for reconfigurable fixtures to minimize the workpiece deformation during machining.[12] A Discrete-Integer GA was developed to optimize fixture layout for minimum deformation. In order to simultaneously optimize fixture arrangement and fixturing sequence, Hajimiri *et al*. used the GA-FEM method.[13] The deformation of the workpiece was calculated using the ABAQUS FEA tool. Rubio-Mateos *et al*. studied the vibration behaviour of low-stiffness components constrained by rubber-based vacuum fixtures.[14] Aderiani *et al*. developed an integrated strategy by optimizing fixture design and tolerance for a sheet metal assembly.[15] The results showed the effectiveness of the approach in terms of manufacturing cost and geometrical quality of the assembly. In the 3-2-1 fixture arrangement, Crichigno *et al*. created a method for improving workpiece position accuracy.[16] It was accomplished by minimizing the locators' structural stiffness in the direction that is tangential to the contact. Do *et al*. optimized the fixture layout in a flexible fixture environment by adopting a method based on geometry.[17] Huamin *et al*. developed a stability-based approach for selecting clamping force to machine a complex workpiece.[18] Bejlegaard *et al*. proposed an approach to design flexible fixture configurations.[19]

It is inferred from the above literature that FEA has been widely employed to predict elastic deformation of the workpiece, and it is integrated with an optimization tool to optimize the fixture layout. Integrating the FEA and optimization tool is also very complex and time-consuming. Hence, the 2D analysis was performed in most of the previously reported research works to reduce the computational effort. Further, ANN-based predictive models were used in fixture layout optimization to reduce the computational effort. A comprehensive ANN model can be developed through a sufficient number of results that FEA obtains. Further, the developed model will be suitable for a specific problem; hence, a new model has to be developed for any variation in workpiece size and machining parameters.

In the present work, a generalized model is developed to analyze the workpiece-fixture system subjected to a machining process. The generalized model is further used to improve the part dimensional quality by distributing the contact forces of the locators uniformly. Fixture layout and clamping forces are considered design variables. The proposed method uses a Rigid Body Model to analyze the workpiece fixture system. It is integrated with GA to obtain a uniform distribution of contact forces during machining by optimizing design variables. The governing equations have been generated to predict the contact force of locators for a particular value of each design parameter. The same equations are also used to develop objective functions and constraints in the optimization process. This method is efficient and simple to model and analyze the response of the workpiece-fixture system to fixture layout. Further, this method has the flexibility to integrate constraints of fixture layout design.

Materials and Methods

Formulation of Workpiece-Fixture Model

The formulation of the optimization model involves planning objectives, design variables, and constraints. The objective of the optimization process is to minimize the variance of the contact force distribution during machining. Hence, developing a comprehensive model to predict contact forces during machining is necessary. This work uses generalized governing equations to represent the workpiece-fixture system to predict the contact forces.

Consequently, the equations are used to model the objective and constraint functions. The optimization model is solved using GA, and the entire process is modelled in MATLAB.

Rigid Body Modelling

The Free Body Diagram (FBD) of the Workpiece–Fixture System (WFS) is developed to analyze the contact forces at locators due to the effect of clamping and machining forces. To simulate the milling process, the WFS is modelled with the Part geometry of a prismatic workpiece size L × W × H. The origin and datum surfaces of the workpiece are planned to meet the tolerance requirement. Locators are positioned in the Primary Datum Plane (PDP), Secondary Datum Plane (SDP) and Tertiary Datum Plane (TDP). The clamps are positioned opposite the datum surfaces to restrict the movement of the workpiece during machining. Fig. 1 depicts the arrangement of the locators, clamps, and cutting tool with the workpiece.

The model is developed to incorporate any number of locators and clamps in the WFS to locate and constrain the workpiece concerning the datum. The locators, clamps and their total count in each plane are detailed below.

L_{P_u} = Locators in the PDP (u=1, 2, ..L_{P_n})
L_{S_v} = Locators in the SDP (v = 1, 2, ..L_{S_n})
L_{T_w} = Locators in the TDP (w=1, 2, ..L_{T_n})
C_{P_t} = Clamps in the plane opposite to the PDP (t = 1, 2, ..C_{P_n})
C_{S_r} = Clamps in the plane opposite to the SDP (r = 1, 2, ..C_{S_n})
C_{T_s} = Clamps in the plane opposite to the TDP (s = 1, 2, ..C_{t_n})
T_{P_q} = Tool Position (q = 1, 2, ..T_{P_n})

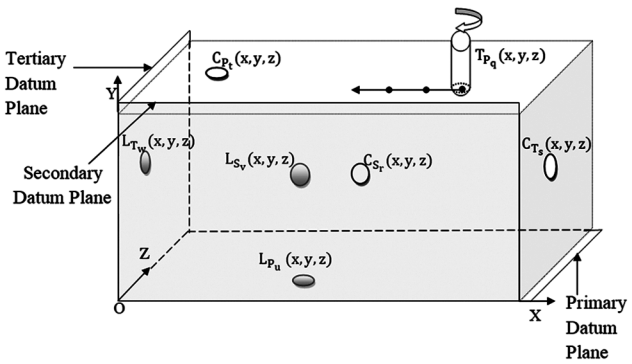

Fig. 1 — Configuration of rigid body model

The workpiece and the fixture elements are modelled by considering a rigid body. Locators support the workpiece, and restricting the movement of the workpiece in the direction normal to the contact surface are considered contact forces. During machining, the workpiece is held in position by applying sufficient force at the contact surface, and it is considered as point force at the workpiece surface in modelling. The nature of machining forces will generally vary based on the machining process. The machining force is measured using a dynamometer, and the components of the same (F_{M_x}, F_{M_y} and F_{M_z}) are incorporated in the modelling along with the tool path appropriately.

The RBM of WFS has been developed in the MATLAB platform to simulate the milling process along with the inputs of workpiece geometry, position of locators, location of clamps, clamping forces, machining forces and tool path. The Free Body Diagram (FBD) is developed using the above inputs. Further, generalized RBM is developed to predict the contact forces at the locator. The numerical values of inputs are fed to the generalized RBM in order to obtain the contact force values at each locator. The various stages involved in developing RBM and predicting contact forces during the machining condition are illustrated in Fig. 2.

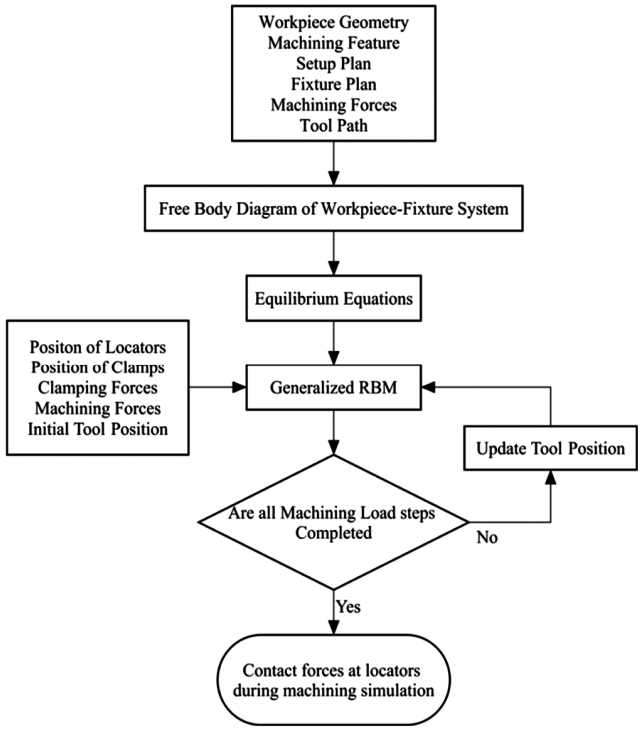

Fig. 2 — Schematic flow diagram for the development of RBM

Input Parameters

The Fixture Plan is essential in developing WFS to analyze and predict contact forces. It includes information such as workpiece geometry, the position of fixturing elements, L_{P_n}, L_{S_n}, L_{T_n}, C_{P_n} and C_{S_n}. The above parameters are used to develop FBD. Consecutively, the RBM is generated with the aid of static equilibrium equations. Clamping and machining forces are necessary input factors for predicting contact forces.

The position vectors of the locators in three different planes, primary, secondary and tertiary are given below in Eqs 1–3, respectively.

$$\overrightarrow{L_{P_u}} = L_{P_u}(x)\,\vec{i} + L_{P_u}(y)\vec{j} + L_{P_u}(z)\vec{k} (u = 1, 2, ..L_{P_n}) \ldots (1)$$

$$\overrightarrow{L_{S_v}} = L_{S_v}(x)\,\vec{i} + L_{S_v}(y)\vec{j} + L_{S_v}(z)\vec{k}\ (v = 1, 2, ..L_{S_n}) \ldots (2)$$

$$\overrightarrow{L_{T_w}} = L_{T_w}(x)\,\vec{i} + L_{T_w}(y)\vec{j} + L_{T_w}(z)\vec{k}\ \ (w = 1, 2, ..\ L_{T_n}) \ldots (3)$$

In general, the clamps are located in the plane opposite to the datum planes. The position vector of the clamps is given below in Eqs 4–6, respectively.

$$\overrightarrow{C_{S_r}} = C_{S_r}(x)\,\vec{i} + C_{S_r}(y)\vec{j} + C_{S_r}(z)\vec{k} \qquad (r = 1, 2, ..C_{S_n}) \ldots (4)$$

$$\overrightarrow{C_{T_s}} = C_{T_s}(x)\,\vec{i} + C_{T_s}(y)\vec{j} + C_{T_s}(z)\vec{k}\ (s = 1, 2, ..C_{T_n}) \ldots (5)$$

$$\overrightarrow{C_{P_t}} = C_{P_t}(x)\,\vec{i} + C_{P_t}(y)\vec{j} + C_{P_t}(z)\vec{k}\ (t = 1, 2, ..C_{P_n}) \ldots (6)$$

The position vector of the self-weight of the workpiece is given by Eq. 7.

$$\overrightarrow{C_g} = C_g(x)\,\vec{i} + C_g(y)\vec{j} + C_g(z)\vec{k} \ldots (7)$$

The position vector of the machining force is based on the location of the cutting tool along the tool path. The machining path is divided into finite numbers, and each segment is considered a load step. The position vector of the machining force at any given load step (q) is provided by Eq. 8.

$$\overrightarrow{T_{P_q}} = T_{P_q}(x)\,\vec{i} + T_{P_q}(y)\vec{j} + T_{P_q}(z)\vec{k} \qquad (q = 1, 2, ...T_{P_n}) \ldots (8)$$

The above inputs and equations are used to develop the workpiece's FBD to facilitate further analysis; the same has been described in the forthcoming section.

Free Body Diagram (FBD) of Workpiece-Fixture System

FBD is used to model WFS by isolating the workpiece from its environment, considering only the forces acting on it. The clamping and machining forces and the contact forces due to the contact of the locators are considered in FBD. Both external and contact forces are considered point forces. The machining process is simulated by changing the position of the moving machining forces along the direction of the tool path in each load step.

In FBD, the number of contact and clamping forces are based on the number of locators and clamps. The following notations are used to express contact and clamping forces to generalize the FBD for any workpiece-fixture configuration.

R_{P_u} = Contact force in the PDP ($u = 1, 2, ..L_{P_n}$)
R_{S_v} = Contact force in the SDP ($v = 1, 2, ..L_{S_n}$)
R_{T_w} = Contact force in the TDP ($w = 1, 2, ..L_{T_n}$)
F_{P_t} = Clamping force in the plane opposite to PDP ($t = 1, 2, ..C_{P_n}$)
F_{S_r} = Clamping force in the plane opposite to SDP ($r = 1, 2, ..C_{S_n}$)
F_{T_s} = Clamping force in the plane opposite to TDP ($s = 1, 2, ..C_{t_n}$)
T_{P_q} = Tool position at various load steps ($q = 1, 2, ..T_{P_n}$)

The configuration of WFS illustrated in Fig. 3 is considered to show the FBD of the workpiece with external and contact forces in Fig. 3.

The entire force system is expressed in vectorial form considering unit vectors along X, Y and Z as $\vec{i}$, $\vec{j}$ and $\vec{k}$. The vectors corresponding to contact forces,

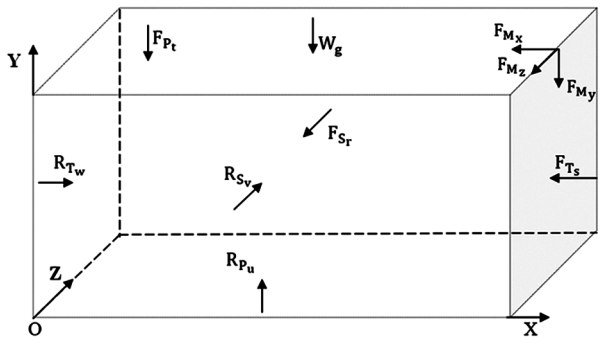

Fig. 3 — FBD of WFS with machining force

clamping forces, components of machining forces and force due to the self-weight of the workpiece have been presented in Table 1. The signs have been accounted for following the usual norms of vectors.

Prediction of Contact Forces

The contact forces at locators due to external forces are essential to be determined to estimate and minimize the contact forces that ultimately help reduce workpiece deformation. It is carried out for each load step. In FBD, the contact forces are evaluated for each load step by applying the equilibrium conditions of summation of forces and moments in all directions as zero. It is to be noted that only six equilibrium conditions are possible, and it is possible to evaluate six unknown contact forces corresponding to each locator. If more than six locators are used, the contact forces of excess locators are assumed as constants by suitably assuming their contact forces.

The contact forces of locators at each machining load step are found by solving the above equations. The equations were obtained by applying the equilibrium conditions ($\Sigma F_x = 0;\ \Sigma F_y = 0;\ \Sigma F_z = 0;\ \Sigma M_{x_o} = 0;\ \Sigma M_{y_o} = 0;\ \Sigma M_{z_o} = 0$) are presented in Table 2. The contact forces corresponding to each locator are determined by solving the six equations in the table. The inverse matrix method is employed for solving the equations obtained using equilibrium conditions. In this method, the coefficients of left and right-hand side parameters are separated and formed as matrix '[A]' and '[B]'. The contact force of locators is called column matrix [X] and is evaluated using the following Eq. 9.

$$[X] = [A]^{-1}\,[B] \quad \ldots (9)$$

Problem Description

The methodology of predicting contact forces is briefed with a pocket milling operation. The pocket milling operations are performed over a prismatic component using an end milling cutter. The prismatic workpiece size 120 × 30 × 40 mm is considered for pocket milling operation. The dimensional details of the prismatic workpiece with its machining features have been illustrated in Fig. 4.

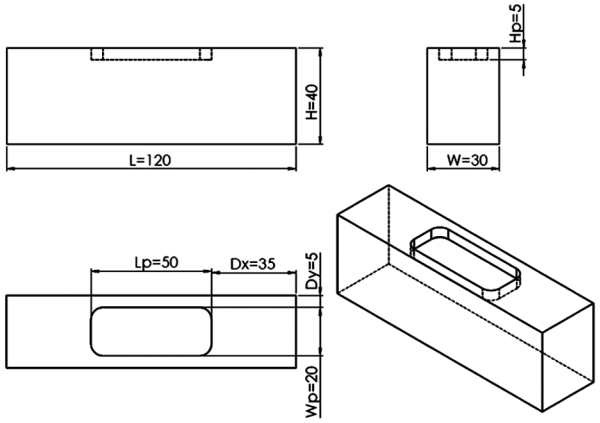

Fig. 4 — Pocket milling features

Table 1 — Force vectors of WFS

S. No	Force vectors	Equation
1	Contact forces	$\overrightarrow{R_{P_u}} = R_{P_u}\vec{j};\ \overrightarrow{R_{S_v}} = R_{S_v}\vec{k};\ \overrightarrow{R_{T_w}} = R_{T_w}\vec{i}$
2	Clamping forces	$\overrightarrow{F_{S_r}} = -F_{S_r}\vec{k};\ \overrightarrow{F_{T_s}} = -F_{T_s}\vec{i};\ \overrightarrow{F_{P_t}} = -F_{P_t}\vec{j}$
3	Machining force at each load step	$\overrightarrow{F_{M_x}} = -F_{M_x}\vec{i};\ \overrightarrow{F_{M_y}} = -F_{M_y}\vec{j};\ \overrightarrow{F_{M_z}} = -F_{M_z}\vec{k}$
4	Self-weight of the workpiece	$\overrightarrow{W_g} = -W_g\vec{j}$

Table 2 — Equilibrium equations of generalized RBM

S. No	Independent equations
1	$\sum_{w=1}^{L_{T_n}} R_{T_w} = \sum_{r=1}^{C_{T_n}} F_{T_s} + F_{M_x}$
2	$\sum_{u=1}^{L_{P_n}} R_{P_u} = \sum_{t=1}^{C_{P_n}} F_{P_t} + W_g + F_{M_y}$
3	$\sum_{v=1}^{L_{S_n}} R_{S_v} = \sum_{r=1}^{C_{S_n}} F_{S_r} + F_{M_z}$
4	$\sum_{u=1}^{L_{P_n}} R_{P_u} L_{P_u}(z) - \sum_{v=1}^{L_{S_n}} R_{S_v} L_{S_v}(y) = -\sum_{r=1}^{L_{S_r}} F_{S_r} C_{S_r}(y) + \sum_{t=1}^{L_{P_t}} F_{P_t} C_{P_t}(z) + W_g C_g(z) + F_{M_y} T_{P_q}(z) - F_{M_z} T_{P_q}(y)$
5	$\sum_{v=1}^{L_{S_n}} R_{S_v} L_{S_v}(x) - \sum_{w=1}^{L_{T_n}} R_{T_w} L_{T_w}(z) = \sum_{r=1}^{C_{S_n}} F_{S_r} C_{S_r}(x) - \sum_{s=1}^{C_{T_n}} F_{T_s} C_{T_s}(z) - F_{M_x} T_{P_q}(z) + F_{M_z} T_{P_q}(x)$
6	$\sum_{u=1}^{L_{P_n}} R_{P_u} L_{P_u}(x) - \sum_{w=1}^{L_{T_n}} R_{T_w} L_{T_w}(y) = -\sum_{s=1}^{C_{T_n}} F_{T_s} C_{T_s}(y) + \sum_{t=1}^{C_{P_n}} F_{P_t} C_{P_t}(x) + W_g C_g(x) - F_{M_x} T_{P_q}(y) + F_{M_y} T_{P_q}(x)$

In pocket milling, the rectangular pocketing of length (Lp) 50 mm and width (Wp) 20 mm is machined to the depth (Hp) of 5 mm in two passes. The pocket feature is oriented using the parameters Dx, Dy and Ds, as illustrated in Fig. 4.

The pocket milling operation is carried out using a two-directional tool path strategy. In contrast to the one-directional strategy, the tool moves forward and reverse. In the present case, the tool makes three parallel motions to machine the pocket's breadth. The pocket depth (Hp) is machined in two tool passes. The distance between the tool's parallel movements is called step over. In the present case, it is considered as 5 mm.

Fixture Arrangement

The fixture arrangement consists of the number of locators and clamps with their positions. It is considered as same for both SM and PM operations. Six locators are considered to locate the workpiece following the 3-2-1 locating principle to constrain the workpiece's movements and rotations. Three locators are placed in the PDP plane and termed as L_{P_1}, L_{P_2} and L_{P_3} respectively. Similarly, the two locators in SDP and one locator in TDP planes are termed as L_{S_1}, L_{S_2} and L_{T_1} respectively. The position of clamps is also termed based on the plane on which it is located. In the present case, three clamps C_{P_1}, C_{S_1} and C_{T_1} are located opposite to PDP, SDP and TDP. The WFS configuration for the prismatic component, along with the locations of the locators and clamps are depicted in Fig. 5.

Prediction of Contact Forces

The simulation of PM operation is carried out to predict the contact forces at the locators using 66 load steps. The pocket width is machined using three parallel movements of the tool in each pass. Each parallel movement of the tool is completed in 11 load steps. The entire depth of the pocket is machined in two passes. The Zeroth load is applied to predict the contact force before the presence of the machining force. The load steps of the PM process are illustrated in Fig. 6 along the tool sequences in each pass.

The equations presented in Table 2 are the generalized equation to determine the contact forces when a number of locators, their positions, clamping forces and machining forces are given as input. In the present numerical example based on a 3-2-1 fixture configuration, the different matrices [A], [B] and [X] are reduced and presented in Eqs 10–12.

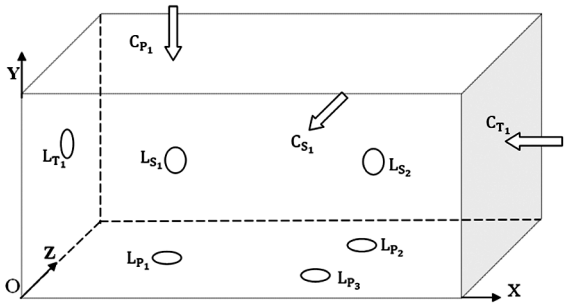

Fig. 5 — Fixture configuration of prismatic workpiece

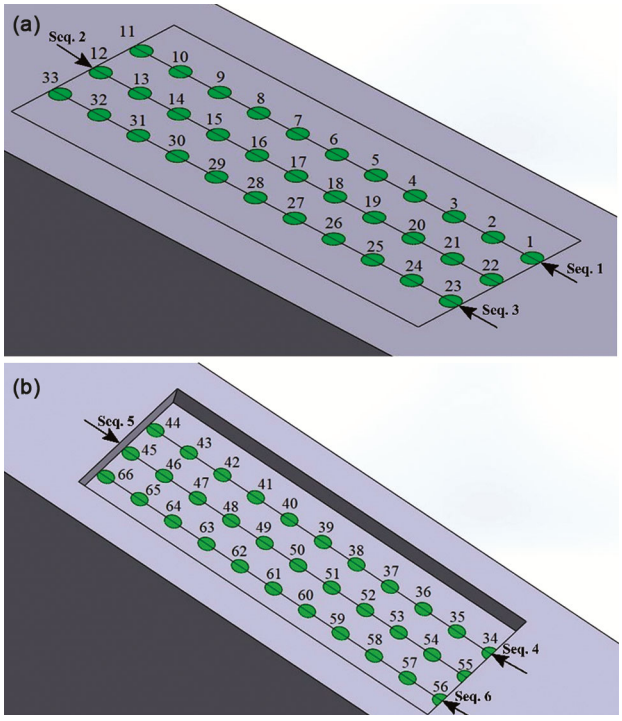

Fig. 6 — Load steps of PM operation in RBM: (a) Tool movement steps during the initial pass, (b) Tool movement steps in the subsequent pass

$$A=\begin{bmatrix} 0 & 0 & 0 & 0 & 0 & 1 \\ 1 & 1 & 1 & 0 & 0 & 0 \\ 0 & 0 & 0 & 1 & 1 & 0 \\ L_{P_1}(z) & L_{P_2}(z) & L_{P_3}(z) & -L_{S_1}(y) & -L_{S_2}(y) & 0 \\ 0 & 0 & 0 & L_{S_1}(x) & L_{S_2}(x) & -L_{T_1}(z) \\ L_{P_1}(x) & L_{P_2}(x) & L_{P_3}(x) & 0 & 0 & -L_{T_1}(y) \end{bmatrix} \quad \ldots (10)$$

$$B = \begin{bmatrix} F_{T_1} + F_{M_x} \\ F_{P_1} + W_g + F_{M_y} \\ F_{S_1} + F_{M_z} \\ -F_{S_1}C_{S_1}(y) + F_{P_1}C_{P_1}(z) + W_gC_g(z) + F_{M_y}T_{P_1}(z) - F_{M_z}T_{P_1}(y) \\ F_{S_1}C_{S_1}(x) - F_{T_1}C_{T_1}(z) - F_{M_x}T_{P_1}(z) + F_{M_z}T_{P_1}(x) \\ -F_{T_1}C_{T_1}(y) + F_{P_1}C_{P_1}(x) + W_gC_g(x) - F_{M_x}T_{P_1}(y) + F_{M_y}T_{P_1}(x) \end{bmatrix} \quad \ldots (11)$$

$$X = \begin{bmatrix} R_{P_1} \\ R_{P_2} \\ R_{P_3} \\ R_{S_1} \\ R_{S_2} \\ R_{T_1} \end{bmatrix} \quad \ldots (12)$$

The positions of fixturing elements, clamping forces, and machining forces are given as inputs. The contact forces shown in the [x] matrix are determined using the inverse matrix method (Eq. 9).

Formulation of Objective Function

Maximizing the uniformity of the contact forces of the locators during machining is essential to improve the machining accuracy. Hence, the objective is to reduce the variance of contact force distribution. The variations among the contact forces are minimized to achieve minimum deformation of the workpiece and ensure form accuracy. The variance of the contact forces is less if the contact forces are uniformly distributed.

The contact forces of all the locators in all load steps and their mean (R_m) are predicted. Subsequently, the variance of the contact forces for the j^{th} fixture layout ($\sigma_{v_j}^2$) of the locators during the machining process simulation is determined using Eq. 13. The objective of the optimization problem is found by Eq. 14.

$$\sigma_{v_j}^2 = \frac{1}{6n_L}\left(\sum_{i=1}^{n_L}((R_{P_{1_k}} - R_m)^2 + (R_{P_{2_k}} - R_m)^2 + \ldots\ldots + (R_{S_{2_k}} - R_m)^2)\right) \quad \ldots (13)$$

$$\{\text{Minimize} \quad \sigma_{v_j}^2\} \quad \ldots (14)$$

The position of the locators and clamps must be varied within its allowable range to achieve the above objective. Each locator and clamp can be fixed at any position within a particular range at accuracy. Further, the clamping loads can also be fixed at any magnitude within its range.

Constraint

The fixture layout design considers two significant constraints concerning interference and stability. The constraints are mathematically modelled and incorporated into the minimization of variation of contact forces, and the same are briefed in the following subsections.

Positional Constraint

The limitations in movement of the locators and clamps are considered positional constraints. The size of the locators and clamps are uniformly taken as 'D'. The fixture–tool and fixture-fixture interferences are considered while modelling positional constraints. The extreme positions of the locators and clamps are termed as Upper Bound (UB) and Lower Bound (LB), respectively. The UB of the clamping forces is determined based on the component of the machining force and its direction. The LB of the clamping forces is considered as zero. The range of the position of each locator and clamp is obtained by considering all the interference constraints.

Stability Constraint

The locator and workpiece must be in contact to ensure the workpiece's stability against external forces. It is achieved by imposing non-negative conditions for the contact forces. The condition of non-negativity for the contact force is given below as Eq. 15 in which the term N_L indicates the number of load steps.

$$R_{P_{1_k}}, R_{P_{2_k}}, R_{T_{1_k}}, R_{S_{1_k}}, R_{S_{2_k}} > 0; \qquad (1 \leq k \geq N_L) \quad \ldots (15)$$

GA-Based Optimization

The solution space of predicting the best fixture layout and a clamping force is increasing exponentially as design parameters are continuous. Hence it is not viable to analyze all possible combinations to predict optimum design parameters. At this juncture, the aid of an evolutionary algorithm is most suitable for selecting the optimum fixture layout and clamping force. In the current work, the optimal fixture design and clamping force were predicted using the Genetic Algorithm (GA). The constraints over the FLD design have also been imposed appropriately to suit the problem for real-world applications.

Each chromosome represents a particular fixture layout and clamping forces in the GA process. It finds the optimum configuration of the fixture and clamping forces by reducing the variance of the contact forces generated during machining. The stability constraint is checked for all possible layouts. The process involved in the optimization procedure has been illustrated as a flow diagram in Fig. 7.

Using GA, the process of determining the optimized fixture configuration that reduces the

variance of the contact forces is carried out. The analogy between the parameters of GA to the present problem environment is described below.

Chromosome

A chromosome is referred to a collection of genes. It represents a unique possible solution to a problem that yields a particular solution concerning the selected objective. In our problem, each chromosome represents a particular fixture layout configuration consisting of the position of locators, clamps and clamping forces. Each position corresponds to genes.

Fitness Function

The contact forces due to locators and clamping forces are fixed when the machining force is applied at any particular position. As the tool advances, the machining force moves along the cutting path; hence, the contact force varies. The objective is to reduce the variance of the contact forces during machining. The minimization of variance of machining force for a chromosome is assigned as the fitness function.

Chromosome and Initial Population

A gene is represented as a design variable in GA. Hence chromosome is the combination of design variables. The initial population is the collection of chromosomes generated randomly within each design variable's range (upper and lower bound). The real values of the design parameters are used in the chromosome.

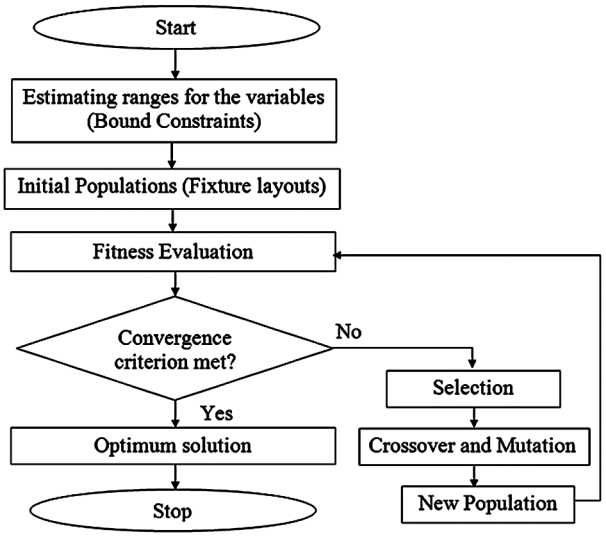

Fig. 7 — GA based optimization procedure

Crossover and Mutation Process

Crossover results in the production of two children by exchanging genes between the chromosomes of the two parents. Every child receives certain traits from each parent. Crossover operators come in a variety of forms. As the chromosomes are real coded, this approach employs a scattered crossover to conduct a crossover operation. In the scattered crossover, the position of the genes will not be interchanged. A random binary vector of ones and zeros is generated using the crossover function. If the value of the vector is "1," then the genes are chosen from the first parent, and if it is "0," then the genes are chosen from the second parent. Consequently, the selected genes are combined to form the child. The second child is formed by doing the same process in vice versa. The process of scattered crossover is illustrated with an example and is presented in Table 3.

The mutation process swaps the genes in the chromosome randomly within the possible range. It avoids the local optimum solutions by ensuring diversity in search.

Formation of New Generation

In this stage, a selection operator is used to choose the definite numbers of the chromosome from the parent and offspring for the next generations.

Termination Criteria

Termination criteria of the GA are set based on the number of generations and the changes in objective function in the successive iteration. The algorithm will terminate and choose the optimal chromosome from the current population if a certain condition is met. If not, it just repeats the cycle of reproduction.

Input for GA

The range of each design parameter is essential to define a chromosome. It is based on the geometry of the workpiece, the dimension of the fixturing elements, clamping forces, cutting forces and the tool movements. The positional restrictions (LB and UB for locators and clamps) of the fixturing elements are outlined in Table 4.

Table 3 — Generation of child from parent chromosomes

Parent	Chromosome	Binary vector	Children
Pa_1	[I J K LM NOP]	[1 1 0 0 1 0 0 0]	[I J 1 7 M 4 5 2]
Pa_2	[98176452]		[98KL 6NOP]

Table 4 — LB and UB of fixturing elements for pocket milling operation

S. No	Fixture Element	LB in mm	UB in mm
1	$L_{P_1}(x)$	5	55
2	$L_{P_1}(z)$	5	25
3	$L_{P_2}(x)$	65	115
4	$L_{P_2}(z)$	20	25
5	$L_{P_3}(x)$	65	115
6	$L_{P_3}(z)$	5	10
7	$L_{T_1}(y)$	5	35
8	$L_{T_1}(z)$	5	25
9	$L_{S_1}(x)$	5	55
10	$L_{S_1}(y)$	5	35
11	$L_{S_2}(x)$	65	115
12	$L_{S_2}(y)$	5	35
13	$C_{T_1}(y)$	5	30
14	$C_{T_1}(z)$	5	25
15	$C_{S_1}(x)$	5	115
16	$C_{S_1}(y)$	5	35
17	$C_{P_1}(x)$	5	35
18	$C_{P_1}(z)$	5	25

The six locators and three clamps have been decided to be used for pocket milling operation following 3-2-1 locating principles by placing three locators in the primary plane, two in the secondary plane and one in the tertiary plane. Three clamps have been employed to secure the workpiece in three different planes. The clamping forces are considered variables and vary from zero to the maximum of machining forces in the corresponding direction. The size of the locators and clamps is considered 5mm.

The initial population is selected by satisfying the constraints such as position and stability. The chromosomes in GA are formulated based on any fixture layout configuration. The initial population in the case of GA is taken as 200. The basic entities are checked for positional and stability constraints before being included in the population. Thus the required number of the initial population is generated for GA implementation. The fitness function value for the chromosomes is evaluated using Eq.13. A sample of the initial population in GA that satisfies the position and stability constraints is presented in Table 5 with the objective function.

The values of contact forces for a single load step is given by Eq. 13. Similarly, the contact forces for all the load steps are found for the corresponding pocket milling operations and illustrated in Fig. 8.

It is noted from the graph that in all the load steps, the contact force values are non-negative, which indicates that the workpiece is stable. It is to be noted that the zeroth load step is performed before the machining process; otherwise, it represents zero machining force.

Table 5 — Chromosome format and sample chromosomes

S.No.	Chromosome Format; Unit	Chromosome −1	Chromosome −2
1	$L_{P_1}(x)$; mm	5	5
2	$L_{P_1}(z)$; mm	5	5
3	$L_{P_2}(x)$; mm	65	85
4	$L_{P_2}(z)$; mm	25	25
5	$L_{P_3}(x)$; mm	65	85
6	$L_{P_3}(z)$; mm	5	5
7	$L_{T_1}(y)$; mm	30	30
8	$L_{T_1}(z)$; mm	10	15
9	$L_{S_1}(x)$; mm	10	10
10	$L_{S_1}(y)$; mm	30	30
11	$L_{S_2}(x)$; mm	90	110
12	$L_{S_2}(y)$; mm	30	30
13	$C_{T_1}(y)$; mm	10	10
14	$C_{T_1}(z)$; mm	10	15
15	$C_{S_1}(x)$; mm	50	60
16	$C_{S_1}(y)$; mm	30	30
17	$C_{P_1}(x)$; mm	20	30
18	$C_{P_1}(z)$; mm	10	10
19	F_{T_1} ; N	160	160
20	F_{S_1} ; N	160	160
21	F_{P_1} ; N	160	160
	Fitness/ Objective Value in N	6186	6168

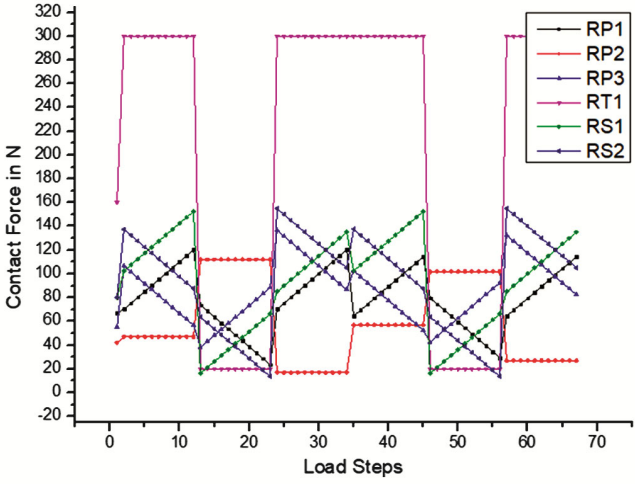

Fig. 8 — Contact force distribution of chromosome-1 for PM

Reproduction Stage in GA

Crossover and mutation operators have been used to reproduce next-generation chromosomes from first-

generation chromosomes. For the next generation, some of the better chromosomes are kept by using the idea of elitism. In this instance, the elite count is 0.05 times the population size.[12] The crossover fraction is taken as 80%.[(12)] It denotes the percentage of chromosomes that aren't part of the elite count and are taken into account during crossover operations. The newly created chromosomes are examined for adherence to restrictions and assessed for their objective function. The next-generation chromosomes are reviewed for compliance with constraints and evaluated for their objective function. Mutation processes are also carried out to randomly change the genes of the chromosome within the positional constraint. The mutation percentage is considered as one percentage.[12] The maximum number generation and solution convergence are termination criteria. The GA provides the optimum fixture layout and clamping force upon satisfying any termination criteria.

Results and Discussion

Several runs have been made in GA; however, only the outcomes of the best five runs are shown in Tables 6 & 7. The optimized fixture layout and clamping forces differed slightly for a few factors, even though the fitness value is similar. The findings show that the fixture problem has several optimum solutions in the search space.[2] It provides flexibility to the tool designer in selecting the fixture designs and clamping forces. In this case study, run 5 in Table 6 is where the global fitness value of 5987 is found. The variation in fitness value with the number of generations is shown in Fig. 9; The convergence reaches in 340 generations. The convergence curve makes it clear that the objective function has greatly improved. Further, a significant reduction in the objective function value is observed from the initial design to the optimum design. The chromosome which was considered the initial design is presented in Table 4. The elitism idea minimizes the number of iterations required to calculate the objective function, despite the high number of generations, by keeping the best solution in each generation.[12]

The trend of contact force distribution for the pocket milling operation is illustrated in Fig. 10. In addition to the position of machining forces during load step simulation, the direction of the machining forces also influences the contact force distribution. It is due to the machining force's direction change during the tool's second parallel movement. Further, it is understood from Fig. 10 that the optimized design does not yield any negative contact force during the machining process. It is because of the effective

Table 6 — Optimized fixture layout for pocket milling process using GA

S. No	Fixture Layout (mm)	Trials of GA				
		1	2	3	4	5
1	$L_{P_1}(x)$	5	5	5	5	5
2	$L_{P_1}(z)$	5	23	25	23	23
3	$L_{P_2}(x)$	65	115	115	115	115
4	$L_{P_2}(z)$	25	25	25	25	25
5	$L_{P_3}(x)$	115	65	65	65	65
6	$L_{P_3}(z)$	10	5	5	5	5
7	$L_{T_1}(y)$	35	35	35	35	35
8	$L_{T_1}(z)$	21	16	15	15	15
9	$L_{S_1}(x)$	5	5	5	5	5
10	$L_{S_1}(y)$	29	35	35	35	35
11	$L_{S_2}(x)$	115	115	115	115	115
12	$L_{S_2}(y)$	35	35	35	35	35
13	$C_{T_1}(y)$	5	5	5	5	5
14	$C_{T_1}(z)$	5	25	5	25	25
15	$C_{S_1}(x)$	42	69	50	70	70
16	$C_{S_1}(y)$	35	35	35	35	35
17	$C_{P_1}(x)$	20	20	20	20	19
18	$C_{P_1}(z)$	20	20	20	20	20

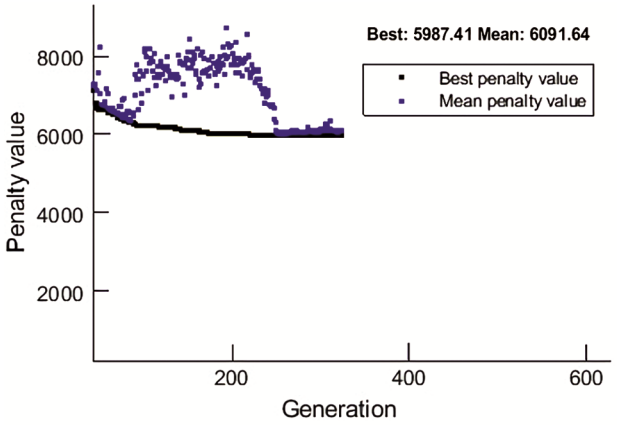

Fig. 9 — GA fitness function convergence curve

Table 7 — Optimized clamping force for pocket milling process using GA

S.No	Clamping Forces (N)	Trials of GA for PM				
		1	2	3	4	5
1	F_{P_1}	150	150	150	150	150
2	F_{S_1}	158	153	152	153	153
3	F_{T_1}	100	100	100	100	100
Objective Function value		6122	5988	5994	5988	5987
Number of runs		30900	27900	28800	29200	30100

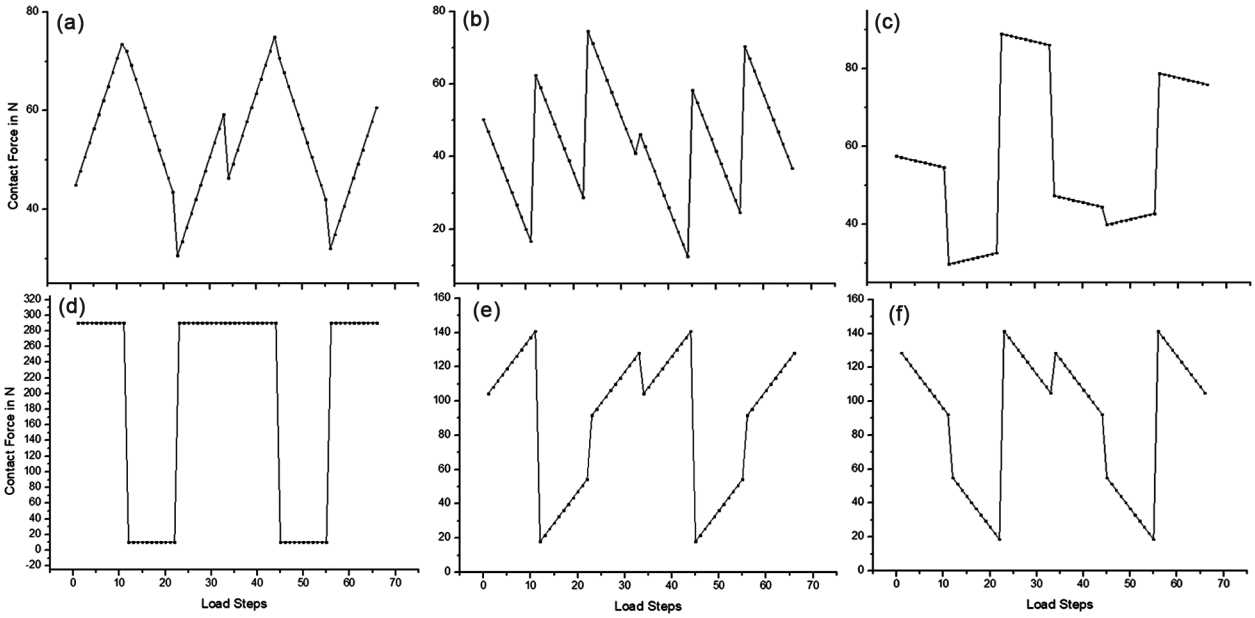

Fig. 10 — Contact force distributions at different load steps of PM: (a) Contact forces at locator L_{P_1}, (b) Contact forces at locator L_{P_2}, (c) Contact forces at locator L_{P_3}, (d) Contact forces at locator L_{T_1}, (e) Contact forces at locator L_{S_1}, (f) Contact forces at locator L_{S_2}

inclusion of stability constraint validation in the optimization process.

Validation of Results using FEM

Finite Element modelling is used to verify the efficacy of the GA-RBM method's findings. The degree of deformation in the workpiece was calculated using the optimal fixture arrangement configuration. The contact force obtained in the rigid body model was correlated with the results of the FEA, and it is revealed that there is a close agreement between the results. The maximum deformation will be obtained in each load step. The critical deformation, which results in form error, is defined as the maximum deformation value across all load steps. The corresponding load step is considered to be a critical load step. The pocket milling process is simulated with 66 load steps by considering the machining force along the tool path. The load steps considered in the PM simulation using RBM are taken for analysis. The machining force simulation considers a length of 5 mm tool travels in each load step. The machining time for each load step is determined as 0.6 seconds.

The deformation of the top edge of the workpiece is determined for each load step, as the top edge deformation contributes to the component's form error. The nodal points at which the deformations noted are taken from Fig. 11. The corresponding

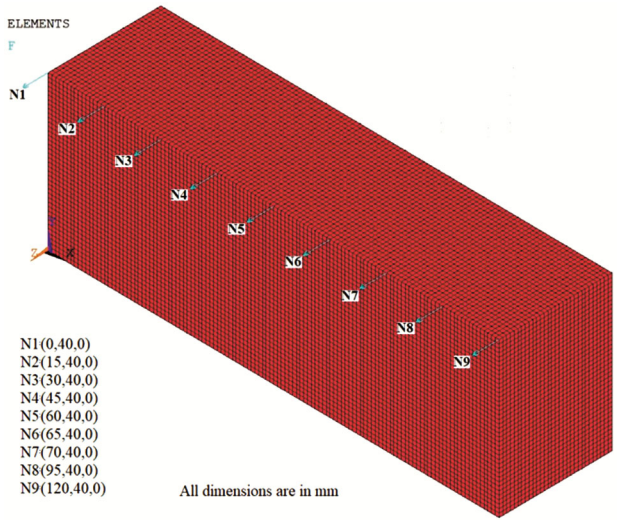

Fig. 11 — Selected nodes for maximum elastic deformation prediction

deformations at nodal points are presented in Table 8.

It is observed from Table 8 that the maximum elastic deformation varies from 3.77 to 5.14 microns. The minimum variation in the maximum deformation during the machining process resulted in good dimensional and form accuracy of the component.[12] The uniformity of the maximum elastic deformation is achieved by reducing the variance of the contact forces during machining. The maximum deformation is obtained on the nodal point 'N_5'. The deformation for all load steps for the nodal point 'N_5' has been

Table 8 — Maximum deformation at various nodal points

S. No	1	2	3	4	5	6	`7	8	9
Node Locations	N_1	N_2	N_3	N_4	N_5	N_6	N_7	N_8	N_9
Maximum Deformation (μm)	3.39	4.12	4.69	4.96	5.12	5.11	4.83	4.33	3.75

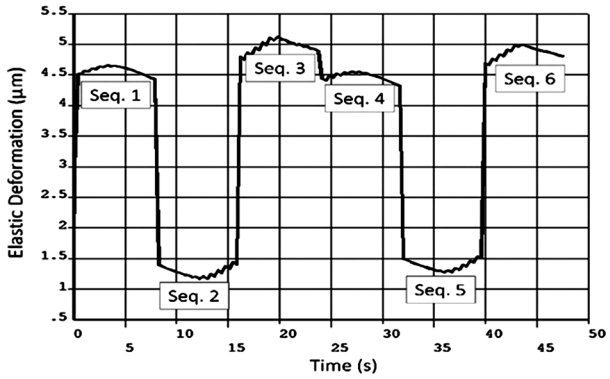

Fig. 12 — Deformation of the workpiece Vs time for the nodal point 'N5'

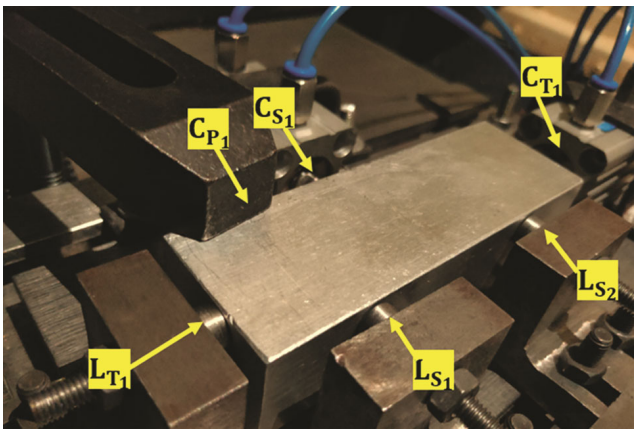

Fig. 13 — Experimental setup

shown in Fig. 12. It is inferred from the graph that the deformation of the workpiece increases for the half sequence and then decreases for the remaining half sequence. As the nodal point, N_5 is located in the mid position of the workpiece; initially, as the tool approaches it, the deformation increases and starts decreasing after the toll moves away from it. During the first pass, the second parallel movement's deformation exhibits less than the other two parallel movements. The reason is attributed to the reversal of the direction of the tool during the second parallel pass. A similar trend has been noticed for the second pass also.

A three-axis machining centre was used for a machining experiment to confirm the viability of the suggested strategy. The workpiece's measurements and the machining settings were identical to those in the numerical analysis. The optimal and first fixture layout combinations were subjected to experimental examination. In Fig. 13, the experimental setup used in this study is depicted. After machining the component, the pocket milling feature's form errors were studied and observed well within the acceptable tolerance.

Conclusion

The presented work introduced a GA and rigid Body Model (RBM) based integrated approach to determine optimum fixture layout and clamping force in milling fixture design. The approach minimizes the variance of the contact force distribution throughout the machining. It also showed that by reducing the variation of contact forces, the workpiece's elastic deformation is minimized, and as a result, the form errors in the completed component are reduced. As the RBM is generalized, it can be used for modelling the workpiece-fixture system of any prismatic component with varying dimensions. The consideration of stability criteria and the elitism concept reduced the iterations in GA by ignoring the impossible fixture configurations and retaining the best fixture configurations. Therefore, the suggested method enables the tool designer to determine the optimal fixture configuration and appropriate clamping force by employing a computationally efficient parametric model and optimization methodology. Although the approach presented in the study was implemented for pocket milling operations, it can also be used for other milling features. It is viable because the generalized RBM is adaptable and enables the tool designer to change the design variables with the existing parametric model.

References

1 Wan M, Dang X Bin, Zhang W H & Yang Y, Chatter suppression in the milling process of the weakly-rigid workpiece through a moving fixture, *J MaterProcess Technol*, **299** (2022) 117293.

2 Kaya N, Machining fixture locating and clamping position optimization using genetic algorithms, *Comput Ind*, **57** (2006) 112–120.

3 Vishnupriyan S, Muruganandam A & Govindarajan L, Prediction of workpiece dynamic motion using an optimized artificial neural network, *Proc Inst Mech Eng Part B J Eng Manuf*, **226** (2012) 1705–1716.

4 Rex F M T & Ravindran D, An integrated approach for optimal fixture layout design, *Proc Inst Mech Eng Part B J Eng Manuf*, **231** (2017) 1217–1228.

5 Ramachandran T, Surendarnath S & Dharmalingam R, Engine-bracket drilling fixture layout optimization for minimizing the workpiece deformation, *Eng Comput*, **38** (2020) 1978–2002.

6 Yang B, Wang Z, Yang Y, Kang Y & Li X, Optimum fixture locating layout for sheet metal part by integrating kriging with cuckoo search algorithm, *Int J Adv Manuf Technol*, **91** (2017) 327–340.

7 Lu C & Zhao H W, Fixture layout optimization for deformable sheet metal workpiece, *Int J Adv Manuf Technol*, **78(1)** (2015) 85–98.

8 Wu D, Wang H, Peng J, Zhang K, Yu J, Zheng X & Chen, Machining fixture for adaptive CNC machining process of near-net-shaped jet engine blade, *Chinese J Aeronaut*, **33** (2020) 1311–1328.

9 Arunraja K M, Selvakumar S & Praveen P, Optimization of welding fixture layout for sheet metal components using DOE, *Int J Product Qual Manag*, **28** (2019) 522–558.

10 Li G, Du S, Huang D, Zhao C & Deng Y, Elastic mechanics-based fixturing scheme optimization of variable stiffness structure workpieces for surface quality improvement, *Precis Eng*, **56** (2019) 343–363.

11 Chen C, Sun Y & Ni J, Optimization of flexible fixture layout using N-M principle, *Int J Adv Manuf Technol*, **96** (2018) 4303–4311.

12 Rex F M T, Hariharasakthisudhan P, Andrews A & Abraham B P, Optimization of flexible fixture layout to improve form quality using parametric finite element model and mixed discrete-integer genetic algorithm, *Proc Inst Mech Eng Part C J Mech Eng Sci*, **236** (2022) 16–29.

13 Hajimiri H, Abedini V, Shakeri M & Siahmargoei M H, Simultaneous fixturing layout and sequence optimization based on genetic algorithm and finite element method, *Int J Adv Manuf Technol*, **97** (2018) 3191–3204.

14 Rubio-Mateos A, Casuso M, Rivero A, Ukar E & Lamikiz A, Vibrations characterization in milling of low stiffness parts with a rubber-based vacuum fixture, *Chinese J Aeronaut*, **34** (2021) 54–66.

15 Aderiani A R, Hallmann M, Wärmefjord K, Schleich B, Söderberg R & Wartzack S, Integrated tolerance and fixture layout design for compliant sheet metal assemblies, *Appl Sci*, **11** (2021) 1–18.

16 Crichigno Filho J M, Ricardo de Medeiros & Pereira Cardoso R A, contribution for increasing workpiece location accuracy in a 3-2-1 fixture system, *Proc Inst Mech Eng Part B J Eng Manuf*, **233** (2019) 1332–1335.

17 Do M D, Son Y & Choi H J, Optimal workpiece positioning in flexible fixtures for thin-walled components, *CAD Comput Aided Des*, **95** (2018) 14–23.

18 Huamin W, Guohua Q, Zhuxi W & Dunwen Z, A workpiece stability-based iterative planning of clamping forces for fixturing layout specification of a complex workpiece, *Int J Adv Manuf Technol*, **103** (2019) 2017–2035.

19 Bejlegaard M, El Maraghy W, Brunoe T D, Andersen A L & Nielsen K, Methodology for reconfigurable fixture architecture design, *CIRP J Manuf Sci Technol*, **23** (2018) 172–18.